

Assessment of Cerebral Blood Flow in Alzheimer's Disease by Spin-Labeled Magnetic Resonance Imaging

David C. Alsop, PhD,* John A. Detre, MD,*† and Murray Grossman, MD†

To evaluate the utility of arterial spin-labeled blood flow magnetic resonance imaging for the detection of cerebral blood flow abnormalities in Alzheimer's disease, arterial spin-labeled blood flow images in 16 contiguous 5-mm axial sections were acquired in 18 patients diagnosed with probable Alzheimer's disease and 11 age-matched controls. Blood flow images from all subjects were transformed to a standard anatomical space for voxel-by-voxel statistical analysis. High quality blood flow images were obtained from all but 1 subject. Statistical analysis demonstrated significant flow decreases relative to control subjects in temporal, parietal, frontal, and posterior cingulate cortices. Increased severity of disease, as measured by Mini-Mental State Examination, correlated with posterior parietal and posterior cingulate decreases but not temporal decreases. Arterial spin-labeled magnetic resonance imaging was found to be an effective tool for characterizing flow decreases accompanying Alzheimer's disease. The absence of ionizing radiation or injection and the ability to obtain high quality anatomical images within the same scanning session make arterial spin labeling an attractive technique for the study of Alzheimer's disease, for the evaluation of pharmacological therapies, and, possibly, for early diagnosis.

Alsop DC, Detre JA, Grossman M. Assessment of cerebral blood flow in Alzheimer's disease by spin-labeled magnetic resonance imaging. Ann Neurol 2000;47:93–100

Functional imaging has demonstrated great promise for the diagnosis, investigation, and early detection of degenerative diseases of the central nervous system such as Alzheimer's disease (AD). Positron emission tomography (PET) imaging in AD has revealed marked hypometabolism in specific areas of temporal, parietal, and frontal cortex^{1,2} as well as in the posterior cingulate cortex.³ Single-photon emission computed tomography (SPECT) using blood flow tracers can also demonstrate decreases.^{4–6} Several studies using these imaging techniques have suggested that AD can be detected at a very early stage, possibly even before the appearance of cognitive deficits.^{7,8} Such studies suggest an important role for functional imaging in future studies of disease progression, in the evaluation of pharmacological treatments, and, potentially, in the routine diagnosis of AD.

Over the past decade, magnetic resonance imaging (MRI) methods have been developed that are sensitive to functional changes and provide resolution and contrast comparable with or exceeding that obtained with nuclear medicine techniques, without the use of ionizing radiation. Images sensitive to blood volume,⁹ blood oxygenation,¹⁰ and blood flow^{11–13} are now being rou-

tinely used for activation studies and the clinical evaluation of stroke¹⁴ and neoplasms.¹⁵ Such MRI techniques could be advantageous for studies of dementia, because MRI is more widely available than PET, has higher spatial resolution than SPECT, and can produce high resolution, spatially coregistered, structural images for quantifying atrophy and ruling out other possible causes of dementia. Blood volume MRI scanning requires the rapid injection of a magnetic contrast agent. Blood volume can be inferred from the amplitude and duration of signal attenuation induced by the agent in the microvasculature. Blood volume imaging has been explored for the study of dementia by several groups.^{16,17}

Blood flow MRI by arterial spin labeling¹² uses electromagnetic labeling of the naturally existing water in the blood to acquire images sensitive to flow without any external contrast agents. Initial implementations for human scanning^{18,19} were limited to single slices and could not provide accurate quantitative flow values. Nevertheless, one preliminary study of AD was able to report significant differences relative to controls.²⁰ Recent technical advances have made the acquisition of multiple slices²¹ and absolute quantification²²

From the Departments of *Radiology and †Neurology, University of Pennsylvania Medical Center, Philadelphia, PA.

Received Sep 28, 1998, and in revised form Jul 27 and Aug 23, 1999. Accepted for publication Aug 27, 1999.

Address correspondence to Dr Alsop, Department of Radiology, University of Pennsylvania Medical Center, 3400 Spruce Street, Philadelphia, PA 19104-4283.

possible. The acquisition of coregistered anatomical images permits the use of automatic computer algorithms to anatomically align the brains of different subjects for three-dimensional (3D) image analysis. Herein, we report the results of a study in which we used quantitative, multislice arterial spin labeling blood flow MRI for the evaluation of AD.

Subjects and Methods

Subject Population

A total of 29 subjects were studied. One of the subjects, a patient with severe dementia, was excluded from further analysis because motion was severe even in the spin echo localizer images. Seventeen of the remaining subjects were patients who were diagnosed with probable AD by criteria of the National Institute of Neurological and Communicative Disorders and Stroke-Alzheimer's Disease and Related Disorders Association (NINCDS-ADRDA).²³ A structural MRI scan demonstrated that there was no other structural abnormality that could explain the patient's symptoms, and the modified Hachinski Ischemia Score was 2 or less in all subjects. None of the patients had any history of head trauma,

primary psychiatric diagnosis (psychosis or depression), stroke, hydrocephalus, or metabolic, infectious, or endocrine cause of declining cognition. Patients who satisfied published criteria²⁴ for frontotemporal dementia were also excluded from the study. The average Mini-Mental State Examination²⁵ (MMSE) for the patient group was 20.8 ± 7.0 , indicating moderate dementia. The remaining 11 subjects were approximately age-matched normal controls recruited from the spouses of the patients as well as by advertisement. Subject information is summarized in Table 1. Signed consent was obtained from all subjects, and the study was approved by the University of Pennsylvania Institutional Review Board.

Magnetic Resonance Imaging

All imaging was performed in a GE Horizon Echospeed 1.5-T MRI scanner (GE Medical Systems, Milwaukee, WI). Patients were imaged while lying supine with their heads inside the product head radiofrequency coil. Foam padding was inserted against the sides of the head and the forehead to minimize patient motion. Subjects were instructed to relax and minimize motion during the scans. Each study began

Table 1. Individual Subject Information

Diagnosis	Age (yr)	Sex (1 = F)	Handedness (1 = R)	MMSE	Total Flow ml/(100 g · min)
Normal	64.0	1.0	—	—	43.1
Normal	75.0	2.0	—	—	35.7
Normal	76.0	2.0	1.0	—	31.8
Normal	75.0	1.0	—	—	34.0
Normal	75.0	2.0	—	—	37.4
Normal	53.0	1.0	1.0	—	36.2
Normal	73.0	2.0	1.0	—	43.5
Normal	64.0	2.0	—	—	35.2
Normal	64.0	1.0	—	—	42.5
Normal	67.0	1.0	1.0	—	46.4
Normal	72.0	2.0	—	—	37.4
Mean	68.9	1.5			38.5
SD	7.2	0.5			4.7
AD	79.0	2.0	1.0	11.0	35.0
AD	80.0	2.0	1.0	29.0	24.9
AD	74.0	1.0	1.0	27.0	36.6
AD	78.0	2.0	1.0	27.0	31.3
AD	74.0	2.0	2.0	7.0	21.7
AD	72.0	1.0	2.0	21.0	28.5
AD	74.0	2.0	1.0	20.0	37.5
AD	73.0	1.0	1.0	6.0	28.2
AD	63.0	1.0	1.0	22.0	44.2
AD	55.0	2.0	2.0	20.0	35.4
AD	77.0	2.0	1.0	24.0	29.0
AD	72.0	2.0	1.0	26.0	31.1
AD	71.0	1.0	—	19.0	47.2
AD	81.0	2.0	1.0	23.0	41.2
AD	75.0	2.0	1.0	25.0	44.4
AD	65.0	1.0	1.0	18.0	29.7
AD	65.0	1.0	1.0	28.0	38.2
Mean	72.2	1.6		20.8	34.4
SD	6.8	0.5		7.0	7.2

F = female; R = right; MMSE = Mini-Mental State Examination (score); AD = Alzheimer's disease.

with a rapid sagittal T1-weighted image to determine patient position. Next, arterial spin labeling blood flow imaging was performed by using methods described below. Finally, high-resolution T1-weighted 3D spoiled gradient echo images were acquired with a repetition time (TR) of 35 msec, an echo time (TE) of 6 msec, a slice thickness of 1.5 mm, a flip angle of 30°, a matrix size of 128 × 256, and a rectangular field of view giving an in-plane resolution of 0.9 × 1.3 mm. These 3D images were acquired for computerized alignment of subjects.

Two separate blood flow image acquisitions of eight 5-mm slices with 5-mm interslice gaps were performed to acquire a total of 16 contiguous 5-mm axial slices. These slices did not provide complete coverage of the brain of each subject; however, the variability between subjects in the placement of the slices permitted the study of group differences within most of the cortex. Images of the most inferior portions of the frontal lobe, and in the portions of the temporal lobe immediately superior to the mastoid sinuses, were often degraded by signal loss and distortion because of the echoplanar acquisition, so concrete conclusions about these regions cannot be made from this study. A rectangular field of view of 24 × 15 cm and a rectangular matrix of 64 × 40 were used for the echoplanar acquisition to provide square pixels of 3.75 mm. Adiabatic electromagnetic labeling was applied at the cervicomedullary junction to invert flowing spins in the carotid and vertebral arteries. A radiofrequency irradiation amplitude of 36 mG and a magnetic field gradient of 0.25 gauss/cm were used.²² Labeled images were subtracted from control images acquired while an amplitude-modulated control irradiation²¹ of either 250 or 125 Hz was applied at the same location as the label, to control for systematic effects unrelated to flow. For both the labeled and control images, the irradiation was stopped 1.5 seconds before the acquisition of the images. This postlabeling delay minimizes any systematic errors due to variations in arterial transit times.²² Because asymptomatic cerebrovascular disease is prevalent in the general elderly population and transit times can be strongly affected by stenosis,²⁶ transit time insensitivity is an important requirement for the quantitative study of dementia. After the delay, echoplanar images were rapidly acquired from the eight slices. Gradient echo echoplanar images with a TE of 22 msec, a receiver bandwidth of ±62.5 kHz, and in-plane resolution of 3.75 mm were used. Labeled and control images were alternately acquired every 4 seconds for 6 minutes to produce a total of 45 image pairs for averaging. In addition to the flow-sensitive imaging, a rapid sequence for mapping the T1 in the slices was performed.²² This sequence, which requires just 2 minutes for eight slices was intended to produce T1 information necessary for quantification of the blood flow-sensitive images. A 1-minute calibration sequence to correct the echoplanar images for distortion and ghosting was also performed.²⁷ The total time for acquiring all images necessary for quantitative blood flow imaging was less than 20 minutes, and the entire examination, from patient entry to exit, was always less than 45 minutes.

Image Analysis

All image data were transferred by digital tape to a Sun Ultra1 workstation for subsequent processing. The blood flow

and T1 echoplanar images were reconstructed from the raw echo amplitudes, using software developed in the IDL analysis environment (Research Systems, Boulder, CO). Because of the rapid interleaving between label and control images, motion artifacts were minimal for most subjects; but to further improve image quality, a motion correction algorithm²⁸ was applied to the individual label and control pairs before averaging. T1 maps were obtained from the T1 scans by nonlinear least squares fitting, as previously described, but we observed that the resulting T1 maps were frequently degraded by motion whereas the motion corrected blood flow scans were not.

Quantification of the spin-labeled blood flow images is possible because the signal measured is simply a competition between the inflow of labeled blood and the decay of the label with the MRI time constant T1. We have previously estimated the efficiency of our labeling of blood water spins to be 96%²⁹ and directly measured the additional inefficiency of the amplitude-modulated control technique.²¹ Total labeling efficiencies of 70% for 125-Hz amplitude modulation and 60% for 250-Hz modulation were assumed for the quantification based on these previous measurements. The sensitivity of the imaging to the presence of water was calibrated by manually selecting a region within the ventricle of each subject as a reference. Quantification requires a value for the relaxation time, T1. We chose to use the T1 of blood instead of the T1 maps, which is equivalent to assuming that the time to pass through the microvasculature and into the tissue is long compared with T1 and the postlabeling delay. The effects of transit times to the voxel and to the tissue on quantification of blood flow, and the reduction of the transit time sensitivity when a postlabeling delay is inserted between labeling and image acquisition, have been discussed extensively in an earlier publication.²² Quantification is insensitive to assumptions about transit times in gray matter, where most of the dementia-related changes are expected, but blood flow in white matter could be underestimated if the assumptions fail. The blood flow images and the 3D T1-weighted images were resampled to a common space of 4-mm resolution.

Images from different subjects were aligned to a standard brain by using the 1996 version of the Statistical Parametric Mapping (SPM) package (Wellcome Department of Cognitive Neurology). The resampled T1-weighted images were used to determine the parameters for transforming to the standard brain. The SPM alignment algorithm uses linear and nonlinear warping to align brain structures.³⁰ The alignment procedure is completely automated and requires no user input. The default SPM values for the alignment were used except that 4-mm resolution was requested. The nonlinear alignment algorithm produced qualitatively good alignment across subjects, but the nonlinear degrees of freedom were insufficient to correct for enlarged ventricles in the more severe cases. The blood flow images were also transformed to the standard space, using the warping parameters of the T1-weighted images. This implicitly assumes that motion between the acquisition of the two scans was minimal. The blood flow images were then smoothed, using a gaussian kernel of 12 mm full width half maximum, in preparation for statistical analysis.

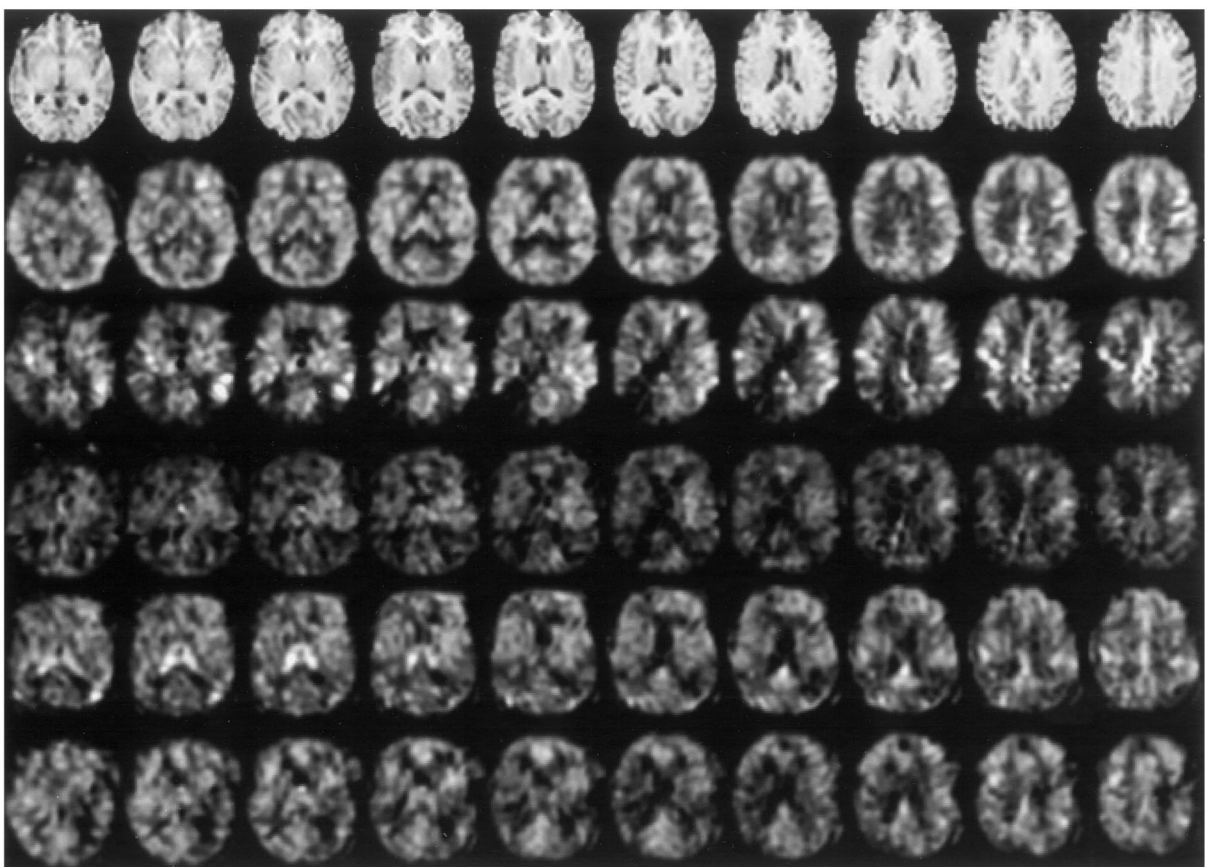
The blood flow images were tested for significant differ-

ences between groups by using an approach similar to the compare groups function of the PET component of the SPM software, but the algorithm was implemented in separate code. This special implementation used a weighting function, which permitted the analysis of regions of the brain where some subjects did not have data because of incomplete slice coverage. A voxel was analyzed as long as at least 7 subjects had valid data at that location. Because of the variability of slice coverage, analysis could be performed in most of the cortex. The flow image of each subject was divided by the flow measured within a region containing the basal ganglia and thalamus. The cerebellar flow, which is frequently used for normalizing functional images, was not available because of the slice coverage of this study. Two statistical analyses were performed on the image data. First, the voxel-by-voxel t statistic was calculated for the difference between patients and control subjects. This statistic was then transformed to a normally distributed z statistic. Second, a linear regression between blood flow in the patients and MMSE score was calculated. The t statistic for a regression coefficient different than 0 was calculated and also converted to a normal distribution. z scores were averaged along 3-cm-long lines of sight into the cortex from eight different viewpoints and corrected for the approximately three independent values along the 3-cm line. The resulting averaged z scores were thresholded at a value of 2.6, which corresponded to $p <$

0.01, of a false-positive uncorrected for multiple comparisons. The thresholded z maps were then overlaid, in color, on top of 3D renderings of the brain supplied with SPM96. The color scale was chosen such that pixels with yellow coloring have z values greater than 3.8, which correspond to a $p < 0.05$ of a false-positive, corrected for multiple comparisons across the two-dimensional projection.³¹ This cortical projection approach to increasing the study sensitivity by decreasing the number of degrees of freedom has previously been reported for analysis of nuclear medicine studies of dementia.³²

A region-based analysis was also performed, to support the statistical methods of the image-based analysis. Regions were manually drawn on T1-weighted images from one of the normal controls after transformation to the standard space. Regions defining the entire temporal, frontal, parietal, and occipital lobes of each hemisphere were drawn following boundaries defined in a published atlas.³³ A region containing the thalamus and basal ganglia was also drawn for normalization of flow. We chose to use whole lobe regions, because they include most of the data but minimize the total number of regions and their definition is less arbitrary than that of smaller regions. Cerebral blood flow in each region was quantified for each subject. Because whole brain data were not obtained, only those voxels with valid data were used in the average. The exact location and number of voxels

Fig 1. Axial blood flow images in a normal elderly subject (second row) and 4 patients with severe Alzheimer's disease (bottom four rows). The anatomical images from the normal subject are shown on top for spatial reference.



used for the average varied between subjects because of different imaged slice positions. An average of the eight lobe values was also calculated as an indicator of whole brain flow. Regional values were tested for significant difference between patients and controls, using the one-sided *t* test, and for significant correlations with MMSE score in the patients, using the *F* statistic of the regression. Significance was calculated for both the flow images and the flow images normalized to the basal ganglia and thalamus flow.

Results

MRI studies produced satisfactory images in all but 1 of the more severe AD subjects, who attempted to rise several times during the course of the scans. This subject was excluded from further analysis. Global and focal flow decreases were clearly apparent in all 4 of the most severe AD patients (Fig 1). The reduced flow in temporal and parietal association cortex is consistent with other studies using PET and SPECT. Flow decreases were more challenging to visually identify in the individual mild AD subjects.

Image-based group analysis produced highly significant results. The volume of the brain covered by the group analysis is shown in Figure 2. This analysis revealed multiple areas of significant blood flow decrease in the AD group relative to controls (Fig 3). Significant decreases were detected in temporal, parietal, and frontal cortex and the posterior cingulate. Also apparent is a significant decrease in the area of the lateral ventricle, which appears to represent loss of white matter flow in this region because of the larger ventricles of the patients. A decrease in flow in the anterior portion of both medial temporal lobes is also apparent. Within the patient group, a significant correlation between MMSE score and perfusion was detected in the temporoparietal association cortex and the posterior cingulate (Fig 4).

Regional analysis of the images produced results that were qualitatively consistent with the image-based analysis. Results obtained with the normalized images were much more significant than with the nonnormalized images. Significant decreases in normalized flow relative to controls were detected in all of the cortical regions. A significant decrease in total cortical flow was also detected. The flow values in the left and right parietal cortex and the left occipital cortex (which includes the posterior cingulate), and the total cortical flow, were significantly correlated with MMSE score. Absolute blood flow values in normal subjects were consistent with earlier studies of older subjects.^{34,35} The fractional decreases in flow observed in the AD patients were also consistent with those measured with SPECT³⁶ and PET.³⁷ Although our fractional decreases appear similar to those obtained with PET imaging of glucose utilization, flow and glucose consumption need not be perfectly coupled. Recently, some

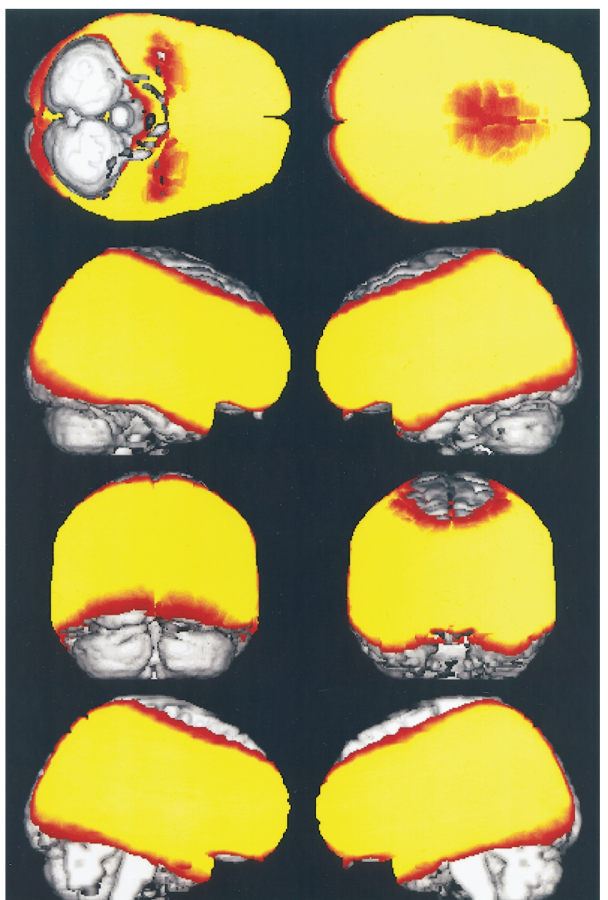


Fig 2. The volume of the brain evaluated in this study. The color scale represents the number of 4-mm voxels with data in at least 7 subjects along a 3-cm deep line into the brain. A three-dimensional rendering of a brain is shown in regions where insufficient data were obtained. The most superior regions of the frontal and parietal lobes and the most inferior regions of the temporal lobes were not evaluated. Imaging artifacts may also compromise the significance of results in the most inferior portions of the frontal lobe.

evidence for decoupling of flow and oxidative metabolism in AD has been reported.³⁷

Discussion

This study conclusively demonstrates that noninvasive blood flow MRI can be used to detect pathological alterations of tissue in suspected AD. The ability to acquire multiple sections made voxel-by-voxel statistical analysis very successful. In addition to the blood flow studies, high-resolution structural images were obtained without moving the subject, making automated registration of patient brains possible. The results of Figures 3 and 4 and Table 2 compare favorably with similar analyses of glucose consumption PET and blood flow SPECT scans.^{6-8,32,38}

The combination of blood flow MRI with anatom-

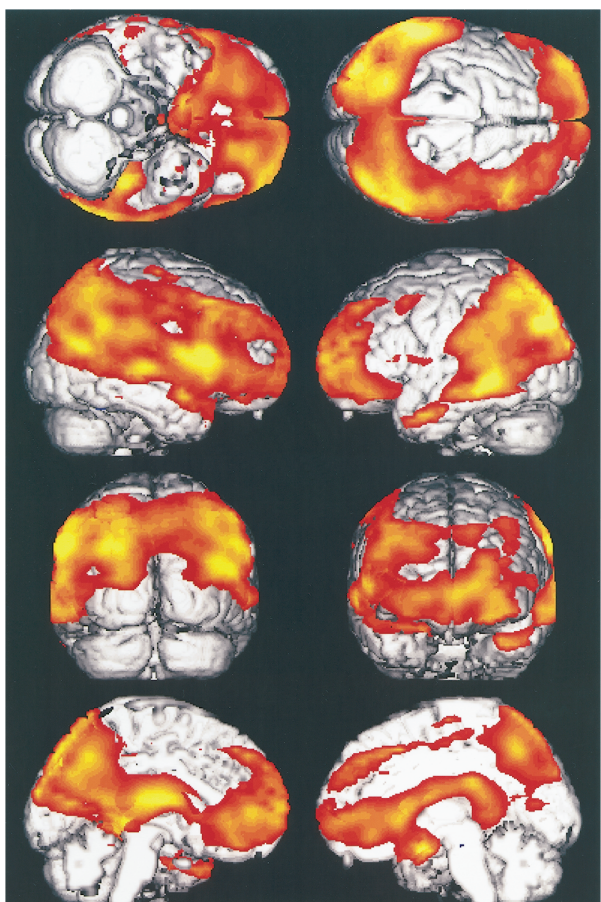


Fig 3. Significant decreases in regional blood flow relative to the control population. Significant results are overlaid in color on top of a surface rendering of the brain. Yellow colors are the most significant and dark red are the least significant.

ical MRI could be a convenient and powerful approach to the clarification of several controversies in dementia research. It has been suggested that the decrease in blood flow and metabolism observed in functional imaging studies such as this one simply represents the loss of metabolically active tissue and its replacement with cerebrospinal fluid. Modern anatomical MRI and segmentation techniques can be used to evaluate the loss of gray matter volume and correlate it with functional imaging findings. Previous investigations^{39,40} have primarily used brain–cerebrospinal fluid segmentation, which ignores the three to four times higher metabolism in gray matter than white matter, and have required registering images of two different modalities. Another area of debate is on the contribution of leukoaraiosis to the observed deficits in demented populations.⁴¹ T2-weighted MRI is ideally suited to the quantification of the defining diffuse white matter lesions of leukoaraiosis and can readily be performed in the same study as blood flow MRI.

Blood flow MRI is but one of several techniques for

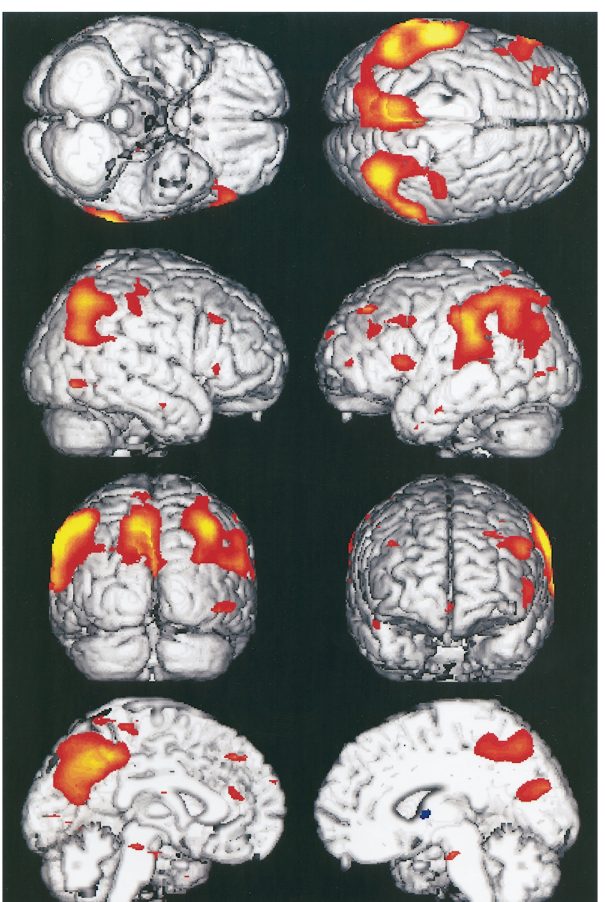


Fig 4. Significant correlations between decreased regional blood flow and severity of disease as measured by the decrease in Mini-Mental State Examination score. Significant results are overlaid in color on top of a surface rendering of the brain. Yellow colors are the most significant and dark red are the least significant.

imaging brain function that have been applied to AD. This technique is most similar to SPECT studies, which also measure blood flow; however, the techniques differ in the systematic errors that can occur. The primary advantages of blood flow MRI are the absence of injection and ionizing radiation, the ease of absolute quantification, and the ability to obtain other types of spatially registered magnetic resonance information. Modern MRI can measure anatomical structure and atrophy, and detect acute and chronic infarcts and even biochemical imbalances. The primary disadvantages of the MRI technique are the low signal-to-noise ratio, which limits the spatial resolution, sensitivity to motion, and systematic underestimation of flow if the transit time from the base of the brain to the tissue is much longer than 1 second. Signal-to-noise ratio can be improved by longer acquisitions, opti-

Table 2. Average Blood Flow in Eight Regions of the Brain for the Control and Patient Populations

	LT	RT	LF	RF	LP	RP	LO	RO	Total Flow
Normal controls	34.6 (5.4)	35.8 (3.2)	37.2 (5.3)	41.6 (6.4)	39.8 (5.3)	41.5 (6.9)	39.4 (7.3)	37.8 (7.3)	38.5 (4.7)
Alzheimer's patients	29.9 (6.9)	32.3 (5.6)	36.0 (7.3)	38.9 (6.9)	34.4 (10.2)	35.4 (8.9)	32.7 (10.0)	35.0 (9.1)	34.4 (7.2)
Significance of nonnormalized difference	0.028	0.024	0.320	0.139	0.039	0.028	0.026	0.188	0.038
Significance of normalized difference	0.00006	0.003	0.011	0.002	0.0008	0.0009	0.002	0.02	0.0006
Significance of nonnormalized MMSE regression	0.290	0.370	0.270	0.396	0.031	0.091	0.065	0.164	0.139
Significance of normalized MMSE regression	0.14	0.13	0.09	0.36	0.002	0.008	0.033	0.10	0.03

Blood flow values are expressed as milliliters per 100 g per minute [ml/(100 g · min)]; SD values are in parentheses. L = left; R = right; T = temporal; F = frontal; P = parietal; O = occipital; MMSE = Mini-Mental State Examination.

mized receiver coils, and higher field strength magnets. In this study, motion during the flow study degraded the images less than during the high-resolution T1 imaging. Although motion can be a problem with very uncooperative patients, the rapid interleaving of labeled and control echoplanar images strongly attenuates motion artifacts.

Blood flow MRI cannot be directly compared with most PET studies of AD because glucose utilization rather than flow is typically measured. Although glucose utilization and flow are usually well coupled in the brain, coupling has not been confirmed for the subtle decreases present early in the progression of AD. Measurement of glucose utilization has the advantage that it is more directly connected to metabolism than blood flow. However, because MRI is much cheaper and more widely available than PET, and because blood flow MRI requires no injections and can be part of a comprehensive study providing multiple image contrasts, it has definite advantages for the study of AD, including routine clinical diagnosis, and the serial evaluation of candidate pharmacological treatments. Measurement of blood flow may also be mechanistically important because widespread degradation of the microvasculature occurs in AD.⁴² Because genetic predisposition to AD also gives predisposition to cerebrovascular disease and amyloid deposits can directly affect vessels, the hypothesis that AD is actually a microvascular disease has been advanced.⁴³ The ability to easily measure flow and potentially other microvascular parameters such as water extraction⁴⁴ with the spin-labeling method can help to explore such hypotheses.

Difficulty detecting medial temporal metabolism decreases in AD relative to age-matched controls has previously been reported.⁴⁵ Our study detected significant decreases in the area of the hippocampus and entorhinal cortex where neurofibrillary pathology is first observed in AD.⁴⁶ Because the decrease in this area was

near the border of the slice coverage of this study and degradation of echoplanar image quality at the base of the frontal and temporal lobes may also have affected the results, we prefer not to emphasize the scientific significance of this decrease. Future work, using blood flow labeling of other MRI sequences⁴⁷ and higher spatial resolution, to more carefully examine these structures, is planned.

This research was supported in part by a Biomedical Engineering Research Grant from the Whitaker Foundation, grants NS01668, AG15116, and NS35867 from the National Institutes of Health, the American Health Assistance Foundation, and the Charles A. Dana Foundation.

References

- Frackowiak RSJ, Pozzilli C, Legg NJ, et al. Regional cerebral oxygen supply and utilization in dementia. *Brain* 1981;104: 753–778
- Haxby JV, Grady CL, Duara R, et al. Neocortical metabolic abnormalities precede nonmemory cognitive defects in early Alzheimer's-type dementia. *Arch Neurol* 1986;43:882–885
- Minoshima S, Foster NL, Kuhl DE. Posterior cingulate cortex in Alzheimer's disease. *Lancet* 1994;344:895
- Jagust WJ. Functional imaging patterns in Alzheimer's disease. *Ann NY Acad Sci* 1996;777:30–36
- Waldemar G. Functional brain imaging with SPECT in normal aging and dementia. *Cerebrovasc Brain Metab Rev* 1995;7: 89–130
- Bartenstein P, Minoshima S, Hirsch C, et al. Quantitative assessment of cerebral blood flow in patients with Alzheimer's disease by SPECT. *J Nucl Med* 1997;38:1095–1101
- Reiman EM, Caselli RJ, Yun LS, et al. Preclinical evidence of Alzheimer's disease in persons homozygous for the epsilon 4 allele for apolipoprotein E. *N Engl J Med* 1996;334:752–758
- Kennedy AM, Frackowiak RSJ, Newman SK, et al. Deficits in cerebral glucose-metabolism demonstrated by positron emission tomography in individuals at risk of familial Alzheimer's disease. *Neurosci Lett* 1995;186:17–20
- Belliveau JW, Rosen BR, Kantor HL, et al. Functional cerebral imaging by susceptibility contrast. *Magn Reson Med* 1990;14: 538–546

10. Ogawa S, Tank DW, Menon R, et al. Intrinsic signal changes accompanying sensory stimulation: functional brain mapping with magnetic resonance imaging. *Proc Natl Acad Sci USA* 1992;89:5951–5955
11. Detre JA, Leigh JS, Williams DS, Koretsky AP. Perfusion imaging. *Magn Reson Med* 1992;23:37–45
12. Williams DS, Detre JA, Leigh JS, Koretsky AP. Magnetic resonance imaging of perfusion using spin inversion of arterial water. *Proc Natl Acad Sci USA* 1992;89:212–216
13. Ostergaard L, Weisskoff RM, Chesler DA, et al. High resolution measurement of cerebral blood flow using intravascular tracer bolus passages. Part I: Mathematical approach and statistical analysis. *Magn Reson Med* 1996;36:715–725
14. Sorensen AG, Buonanno FS, Gonzalez RG, et al. Hyperacute stroke: evaluation with combined multisector diffusion-weighted and hemodynamically weighted echo-planar MR imaging. *Radiology* 1996;199:391–401
15. Aronen HJ, Gazit IE, Louis DN, et al. Cerebral blood-volume maps of gliomas: comparison with tumor grade and histologic findings. *Radiology* 1994;191:41–51
16. Gonzalez RG, Fischman AJ, Guimaraes AR, et al. Functional MR in the evaluation of dementia: correlation of abnormal dynamic cerebral blood volume measurements with changes in cerebral metabolism on positron emission tomography with fluorodeoxyglucose. *AJNR Am J Neuroradiol* 1995;16:1763–1770
17. Harris GJ, Lewis RF, Satlin A, et al. Dynamic susceptibility contrast MRI of regional cerebral blood volume in Alzheimer's disease. *Am J Psychiatry* 1996;153:721–724
18. Roberts DA, Detre JA, Bolinger L, et al. Quantitative magnetic resonance imaging of human brain perfusion at 1.5 T using steady-state inversion of arterial water. *Proc Natl Acad Sci USA* 1994;91:33–37
19. Edelman RR, Siewert B, Darby DG, et al. Qualitative mapping of cerebral blood flow and functional localization with echo-planar MR imaging and signal targeting with alternating radio frequency. *Radiology* 1994;192:513–520
20. Sandson TA, O'Connor M, Sperling RA, et al. Noninvasive perfusion MRI in Alzheimer's disease: a preliminary report. *Neurology* 1996;47:1339–1342
21. Alsop DC, Detre JA. Multisector cerebral blood flow MR imaging with continuous arterial spin labeling. *Radiology* 1998; 208:410–416
22. Alsop DC, Detre JA. Reduced transit-time sensitivity in non-invasive magnetic resonance imaging of human cerebral blood flow. *J Cereb Blood Flow Metab* 1996;16:1236–1249
23. McKhann G, Drachmann D, Folstein M, et al. Clinical diagnosis of Alzheimer's disease: report on the NINCDS-ADRDA work group under the auspices of the Department of Health and Human Services Task Force on Alzheimer's disease. *Neurology* 1984;34:939–944
24. Grossman M, Desposito M, Hughes E, et al. Language comprehension profiles in Alzheimer's disease multi-infarct dementia, and frontotemporal degeneration. *Neurology* 1996;47: 183–189
25. Folstein MF, Folstein SF, McHugh PR. Mini Mental State: a practical method for grading the cognitive state of patients for the clinician. *J Psychiatr Res* 1975;12:189–198
26. Detre JA, Alsop DC, Vives LR, et al. Noninvasive MRI evaluation of cerebral blood flow in cerebrovascular disease. *Neurology* 1998;50:633–641
27. Alsop DC. Correction of ghost artifacts and distortion in echo-planar MR imaging with an iterative image reconstruction technique. *Radiology* 1995;177P:388 (Abstract)
28. Alsop DC, Detre JA. Reduction of excess noise in fMRI using noise image templates. In: Proceedings of the International Society for Magnetic Resonance in Medicine Fifth scientific meeting and exhibition. Berkeley, CA: International Society for Magnetic Resonance in Medicine, 1997:1687 (Abstract)
29. Maccotta L, Detre JA, Alsop DC. The efficiency of adiabatic inversion for perfusion imaging by arterial spin labeling. *NMR Biomed* 1997;10:216–221
30. Friston KJ, Ashburner J, Frith CD, et al. Spatial registration and normalization of images. *Hum Brain Mapp* 1995;2:165–189
31. Friston KJ, Frith CD, Liddle PF, Frackowiak RSJ. Comparing functional (PET) images: the assessment of significant change. *J Cereb Blood Flow Metab* 1991;11:690–699
32. Burdette JH, Minoshima S, Borght TV, et al. Alzheimer disease: improved visual interpretation of PET images by using three-dimensional stereotaxic surface projections. *Radiology* 1996;198:837–843
33. Hanaway J, Woolsey TA, Gado MH, Roberts MP. The brain atlas: a visual guide to the central nervous system. Bethesda: Fitzgerald Science Press, 1998
34. Gur RC, Gur RE, Obrist WD, et al. Age and regional cerebral blood flow at rest and during cognitive activity. *Arch Gen Psychiatry* 1987;44:617–621
35. Martin AJ, Friston KJ, Colebatch JG, Frackowiak RSJ. Decreases in regional cerebral blood flow with normal aging. *J Cereb Blood Flow Metab* 1991;11:684–689
36. Messa C, Perani D, Lucignani G, et al. High resolution technetium-99m-HMPAO SPECT in patients with probable Alzheimer's disease: comparison with fluorine-18-FDG PET. *J Nucl Med* 1993;35:210–216
37. Nagata K, Buchan RJ, Yokoyama E, et al. Misery perfusion with preserved vascular reactivity in Alzheimer's disease. *Ann NY Acad Sci* 1997;826:271–281
38. Minoshima S, Frey KA, Koeppe RA, et al. A diagnostic approach in Alzheimer's disease using 3-dimensional stereotaxic surface projections of fluorine-18-Fdg Pet. *J Nucl Med* 1995;36:1238–1248
39. Alavi A, Newberg AB, Souder E, Berlin JA. Quantitative analysis of PET and MRI data in normal aging and Alzheimer's disease: atrophy weighted total brain metabolism and absolute whole brain metabolism as reliable discriminators. *J Nucl Med* 1993;34:1681–1687
40. Meltzer CC, Zubieta JK, Brandt J, et al. Regional hypometabolism in Alzheimer's disease as measured by positron emission tomography after correction for effects of partial volume averaging. *Neurology* 1996;47:454–461
41. Gijn JV. Leukoaraiosis and vascular dementia. *Neurology* 1998; 51:S3–S8
42. Buee L, Hof PR, Bouras C, et al. Pathological alterations of the cerebral microvasculature in Alzheimer's disease and related dementing disorders. *Acta Neuropathol (Berl)* 1994;87:469–480
43. Hachinski V, Munoz DG. Cerebrovascular pathology in Alzheimer's disease: cause, effect or epiphénoménon. *Ann NY Acad Sci* 1997;826:1–6
44. Silva A, Zhang W, Williams D, Koretsky A. Estimation of water extraction fractions in rat brain using magnetic resonance measurement of perfusion with arterial spin labeling. *Magn Reson Med* 1997;37:58–68
45. Jagust WJ, Eberling JL, Richardson BC, et al. The cortical topography of temporal lobe hypometabolism in early Alzheimer's disease. *Brain Res* 1993;629:189–198
46. Braak H, Braak E. Neuropathological staging of Alzheimer-related changes. *Acta Neuropathol (Berl)* 1991;82:239–259
47. Alsop DC, Detre JA. Background suppressed 3D RARE arterial spin labeled perfusion MRI. In: Proceedings of the International Society for Magnetic Resonance in Medicine Seventh scientific meeting and exhibition. Berkeley, CA: International Society for Magnetic Resonance in Medicine, 1999 (Abstract)